Smart Hydrophobic-Hydrophilic Self-Switching Cellulosic Materials Synthesized by Regioselective Functionalization

Meiyan Lin, Kunfeng Xia, Pengbo Lu, Yanghao Ou, Lingfeng Su, and Detao Liu *

Smart hydrophobic-hydrophilic self-switching cellulosic materials were synthesized by regioselective functionalization of cellulose in green Ionic Liquids (ILs). The thermal analysis indicated that the introduction of a macromolecular structure including a trityl or heptafluorobutyric group onto the cellulose chain increased the thermal stability of the cellulose derivatives. Wetting contact angle of the surface decreased from 103° to 73° as the holding time increased at ambient conditions (19.8 °C, 65%). After wetting, the surface free energy increased from 11.03 to 34.09 J·m, of which the polarity component increased from 60.92% to 94.19%. The XPS analysis indicated that the content of oleophobic-hydrophobic CF3-CF2-CF2-CO- groups at the exposed surface decreased after wetting, while the hydrophilic HOOC- groups increased, which verified the self-switching process between the hydrophobic and hydrophilic properties within the cellulosic materials. The self-switching characteristic means that the biodegradable cellulosic materials have suitable selectivities for high-impact applications in various fields.

Keywords: Self-switchable process; Ionic liquids; Cellulose; Trityl group; Hydrophobic-hydrophilic process

*Contact information: State Key Laboratory of Pulp and Paper Engineering, South China University of Technology, Guangzhou 510640, China; *Corresponding author: dtliu@scut.edu.cn*

INTRODUCTION

Sustainability, self-responsiveness, and green chemistry are directing the next generation development of switchable functional materials (Godeau *et al.* 2016; Long *et al.* 2016). Typically, conventional self-switchable hydrophobic-hydrophilic materials are synthesized using inorganic materials or synthetic polymers, which have been altered by ultraviolet (UV) irradiation, F4 microwave plasma treatment, pH changes, *etc.* (Van Oss 1995; Iriyama 2010; Sawada *et al.* 2010; Yue *et al.* 2015; Ryu *et al.* 2016; Yuan *et al.* 2016). For example, Ryu *et al.* (2016) used an aluminum substrate that was etched with HCl and subsequently coated with a functionalized poly(NIPAM-co-MAA) polymer; the coated metal surface was self-switchable from hydrophobic to hydrophilic by changing the temperature, and the resulting material was used in an evaporator core of an automobile air conditioner. Yuan *et al.* (2016) reported that the hydrophilic-hydrophobic switching for a graft copolymer film was achieved through heating or cooling the copolymers to the lower or upper critical solution temperatures. Sawada and co-workers (2010) reported that the water wettability of fluorinated oligomer/titanium oxide nanocomposites was self-switchable between superhydrophobic and superhydrophilic by alternately applying UV radiation and dark storage. Compared to these typical polymers, biopolymers have been reported to be superior in terms of their synthesis, environmental sustainability, and wide

availability (Klemm *et al.* 2005; Raghavanpillai *et al.* 2012). In this regard, biodegradable cellulose has received considerable attention in that it has an ideal molecular skeleton for preparing amphoteric materials with its hydroxyl groups at C-6, C-2, and C-3 positions (Luby *et al.* 2003; Shen and Gnanakaran 2009). It is also easy to modify chemically, and it is derived from a sustainable chemical feedstock (Pinkert *et al.* 2010). Usually, regioselective modifications of cellulose are regarded as diversified and easily scalable when achieving smart cellulosic material (Tsunashima *et al.* 2001; Liu *et al.* 2008). However, the modification systems for cellulose over the past several decades has tended to be inefficient due to an inappropriate solvent system (Roy *et al.* 2009). With the development of modern solvent systems, the dissolution and modification of cellulose have become prevailing and practical by destroying its highly ordered structure and strong hydrogen bonds (Heinze and Liebert 2001; Koschella *et al.* 2006; Fox *et al.* 2011). For example, ionic liquids (ILs) have been reported to have tremendous potential for cellulose modification, as these solvents provide milder conditions to dissolve the crystalline structure of cellulose (Vitz *et al.* 2009; Gupta and Jiang 2015).

In general, cellulose derivatives that are regioselectively functionalized can be synthesized with or without protecting group methods (Wang *et al.* 2006; Kamitakahara *et al.* 2010; Liu *et al.* 2012). The former method uses functional groups to block reactive sites (*e.g.,* C-6 hydroxyl group) of cellulose in order to precisely control future derivatization of the cellulose structure. The latter method introduces reagent that only attacks the objective hydroxyl group(s) (*e.g.* C6-OH) without any protecting group (Zhang *et al.* 2010; Tang *et al.* 2012; Zheng *et al.* 2015).

The present work reports a method to prepare smart hydrophobic-hydrophilic self-switching cellulosic material by regioselective functionalization of cellulose by using protecting trityl groups. Trityl chloride meets the requirements of selective introduction, stability during subsequent reactions, and easy removability without influence on other substituents in a homogeneous IL medium. The IL not only provides milder conditions for efficiently dissolving cellulose and regioselectively blocking C6-OH of cellulose, but also achieves higher degrees of distribution (DS) (Granström *et al.* 2009; Pinkert *et al.* 2009). In addition, it is hoped that this study will shed some light on the production of environmentally sustainable and degradable cellulose that have been derivatized to provide hydrophobic-hydrophilic surfaces. The derivatized biopolymer could be potentially fabricated as self-cleaning materials or functional filters, replacing the typical oleophobic–hydrophobic products used in air conditioners for rooms or cars, and reducing global dependence on chemical feedstock derived from petrochemical resources.

EXPERIMENTAL

Materials

Cellulose (99% purity, medium size), DMSO (99.5% purity), tetrahydrofuran (99.5% purity), and trityl chloride (97% purity) were purchased from Sigma-Aldrich Trading Co., Ltd. (Shanghai, China). Pyridine (99.5% purity) was purchased from Chinasun Specialty Products Co., Ltd. (Jiangsu, China). Toluene (99.5% purity; 0.865 to 0.869 g/mL density) was purchased from Hengyang Kaixin Chemical Regent Co., Ltd. (Hunan, China). Heptafluorobutyryl chloride (98% purity; 1.556 g/mL density) was obtained from Alfa Aesar Chemical Co., Ltd. (Shanghai, China). Sodium chloroacetate (98% purity) was purchased from J & K Scientific Ltd. (Guangzhou, China). 1-Butyl-3-methylimidazolium

chloride ([Bmim]Cl) (99% purity; less than 105 ppm water) was purchased from Henan Lihua Pharmaceutical Co., Ltd. (Henan, China). Other chemical reagents were purchased from various commercial suppliers, and were used without further purification unless otherwise specified.

Synthesis of 6-*O*-Trityl Cellulose

6-*O*-Trityl cellulose was synthesized as follows. A sample of cellulose (7.5 g) was dispersed into 65 g [Bmim]Cl using a magnetic stirrer; the cellulose was completely dissolved in this IL with heating at 100 °C. Pyridine (55.89 mL) was added dropwise to the solution under an argon gas atmosphere at room temperature in a 500 mL glass-lined reactor. Afterwards, trityl chloride (50.508 g) was added to the mixture and dispersed. The optimum ratio of the reagents was 1 equiv. cellulose, 9 equiv. trityl chloride, and 15 equiv. pyridine. The reaction mixture was continuously stirred with a magnetic stirrer at 100 °C in a Schlenk flask. The chemical reaction was terminated after 6 h. The resulting tritylated derivatives from the reaction were purified by washing the samples with an excess amount of methanol. The resulting precipitates were repeatedly washed with an excess amount of methanol and vacuum-dried at 60 °C for 24 h yielding 6-*O*-trityl cellulose (product 1).

Synthesis of 6-*O*-Trityl-2,3-*O*-Acetate Cellulose Ester

Product 1 **(**4.04 g) was dissolved in 100 mL of DMSO at 45 °C. After the dissolution of tritylated cellulose, anhydrous NaOH (5.0 g) was added to the dispersion that was kept at room temperature for 4 h. Sodium chloroacetate (8.15 g) was added to this mixture in two steps. In the first step, 7.00 g sodium chloroacetate mixed with 25 mL of DMSO was added to the product 1 solution mixture. The resulting mixture was continuously mixed with a magnetic stirrer at 70 °C for 20 h. In the second step, another 1.15 g sodium chloroacetate mixed with 25 mL of DMSO was added to the resulting reaction mixture. The reaction continued at 70 °C for another 4 h. The resulting derivatized cellulose product was repeatedly washed by large amounts of deionized (DI) water until neutral pH was achieved; afterwards, the washed solids were vacuum-dried at 80 °C for 24 h, which afforded 6-*O*-trityl-2,3-acetate cellulose (product 2). This procedure was repeated four times to prepare enough product 2 for the next synthetic step.

Synthesis of 2,3-*O*-Sodium Acetate Cellulose Ester

In a typical detritylation procedure (Schaller and Heinze 2005), 12.0 g product 2 was dispersed into a 200 mL of ethanol at room temperature under an argon gas atmosphere. Subsequently, 12.0 mL of HCl (36.5% concentration) was added dropwise to the ethanol dispersion. The reaction mixture was continuously stirred with a magnetic stirrer at room temperature for 24 h. After complete detritylation, the resulting precipitate was repeatedly washed with an excess amount of methanol; the washed precipitate was vacuum-dried at 50 °C for 24 h. The dried precipitate was dispersed into a 200 mL of ethanol that contained 7.0 g anhydrous NaOH. The mixture was stirred at room temperature for 18 h. Afterwards, the resulting precipitate was repeatedly washed with an excess amount of methanol, which was then vacuum-dried at 50 °C for 24 h to afford 2,3-sodium acetate cellulose ester (product 3).

Synthesis of 6-*O*-Heptafluorobutyric acid-2,3-*O*-Sodium Acetate Cellulose Ester

A fluorinated derivative of product 3, 6-*O*-heptafluorobutyric acid-2,3-*O*-sodium acetate cellulose ester (product 4) was synthesized by the following procedure. Product 3 (0.5 g) was dispersed in 37.5 mL of anhydrous toluene that contained 3.125 g pyridine. The resulting mixture was further mixed at 80 °C for 1 h. The reaction mixture was then cooled to room temperature. To this mixture was added a total of 1.22 mL of heptafluorobutyryl chloride in two steps. In the first step, 1.0 mL of heptafluorobutyryl chloride was added dropwise to the toluene mixture under an argon gas atmosphere at room temperature in a 250 mL glass-lined reactor. The reaction was continuously stirred with a magnetic stirrer at 100 °C for 2 h. In the second step, 0.22 mL of heptafluorobutyryl chloride was then added to the reaction mixture with stirring, which was allowed to and react further for 2 h. Afterwards, the resulting mixture was repeatedly washed large amounts of DI water, and the resulting washed precipitate was vacuum-dried at 80 °C for 24 h to afford product 4.

Fabrication of Hydrophobic-Hydrophilic Switching Cellulosic Materials (HHSCMs)

HHSCMs samples were produced through pressing the final product of synthesis into a sheet with 15 mm diameter sizes by cold-pressing at 20.0 MPa. The resulting samples were kept under a dried atmosphere.

Characterizations

The chemical structures of products 1, 2, 3, and 4 were characterized by Fourier transform infrared spectra (FT-IR) analysis using a Thermo Nicolet Nexus 470 FT-IR spectrophotometer (Thermo Fisher Scientific (Waltham, MA, USA)). The samples were pressed into standard KBr pellets prior to recording their FT-IR spectra. Each spectrum was recorded using 32 scans over the 4000 to 400 cm^{-1} wavenumber range with a resolution of 4 cm^{-1}.

Further chemical structural information of product 4 was characterized by solid-state ^{13}C MAS NMR analysis on an AVANCE AV 400 (Brüker (Fällanden, Switzerland)) at 100.61 MHz. The 90° pulse width was 3.3 μs, the relaxation delay was 2 s and the data acquisition time was 17.3 μs. The number of scans used to obtain the spectra was 2500.

The hydrophobic-hydrophilic switching process was observed using dynamic contact angle analysis with a Dataphysics OCA40 Micro (Dataphysics (Filderstadt, Germany)). The contact angle measurements ranged from 0° to 180° with an accuracy of ±0.1°. The measurements were recorded at 65% relative humidity and 25±0.1 °C. The HHSCMs samples were fixed to a metal base specimen holder using double-sided tape. Dynamic contact angles were continuously recorded every 1 to 3 min after DI water was positioned onto the HHSCM surface to observe the hydrophobic-hydrophilic switching process of the material. Additionally, oleophobic dynamic contact angles were also recorded using CH_2I_2 that was positioned onto the HHSCM surface. Three determinations have been performed. According to Young's equation, the surface free energy was calculated from the contact angle using the approach of Owens-Wendt-Rabel-Kaelble (OWRK) (Owens and Wendt 1969; Rudawska and Jacniacka 2009).

To verify the mechanism of hydrophobic-hydrophilic switching process, X-ray photoelectron spectroscopy (XPS) analysis was performed with a Kratos Axis Ultra (DLD)

(Kratos Analytical Ltd. (Manchester, UK)). The vacuum pressure used was 5×10^{-9} Torr, and scan mode was CAE with an Al *Kα* X-ray source.

Thermal stability of this material was ascertained by TGA-DTA studies using STA 449 C Jupiter® synchronous thermal analyzer (NETZSCH (Germany)) and TENSOR 27 infrared spectrometer (Brüker (Germany)).

RESULTS AND DISCUSSION

Synthesizing Process and Proposed Mechanism

Cellulose, a homopolysaccharide that consists of anhydroglucose units connected by (1→4)-*β* glycosidic bonds, has received considerable attention in that it has desirable chemical and biodegradable properties. The preparation of the final product 6-*O*-heptafluorobutyric acid-2,3-*O*-sodium acetate cellulose ester is shown in Fig. 1a.

The ILs provide milder conditions for efficiently dissolving cellulose, while the trityl chloride is used to block HO-6 groups in cellulose in order to fully derivatize the HO-2 and HO-3 groups with -CH_2-COONa. After the first derivatization, CF_3-CF_2-CF_2-COOCl is then reacted with the modified cellulose, after detritylation, to derivatize the hydroxyl group at the C-6 position.

As shown in Figure 1b, the oleophobic-hydrophobic CF_3-CF_2-CF_2-CO- groups are attached to the cellulose biopolymer at HO-6, while the hydrophilic HCOO- groups are attached to HO-2 and HO-3, which results in a material with hydrophobic groups on one side and hydrophilic groups on the opposite side. When the external environment is in an ideal state, the spatial orientation of CF_3-CF_2-CF_2-CO- and HCOO- groups are in a state of order-disorder (*i.e*., ideal model).

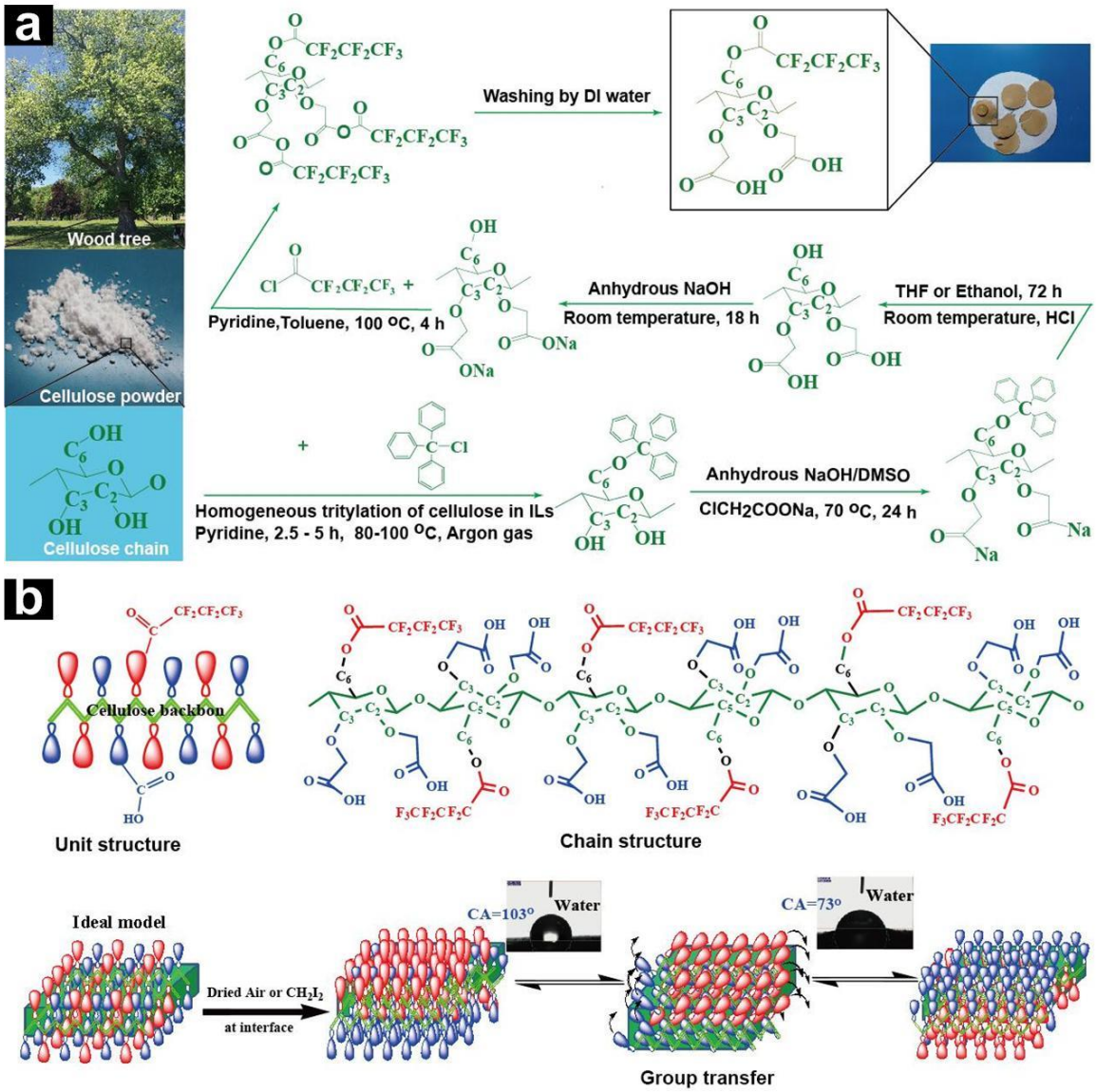

Fig. 1. (a) Synthesizing process; (b) Proposed mechanism of this material

When the external environment is exposed to air, the CF_3-CF_2-CF_2-CO- groups will orientate themselves to the air-polymer interface to lower the surface tension, while the HCOO- groups orientate themselves towards the inner space of the polymer. As a result, the polymer's outer surfaces become oleophobic-hydrophobic. In this state, the initial surface contact angle is 103°. When the external environment changes from air to water, the hydrophilic HCOO- groups inside the material rapidly migrate to the polymer's surface due to the favorable intermolecular force interactions (*e.g.*, van der Waals and hydrogen bonding forces); likewise, the oleophobic-hydrophobic CF_3-CF_2-CF_2-CO- groups migrate to the inner spaces of the polymer. When external environment changes again, the two different groups at the polymer's surface reorient themselves in the most favorable configuration, which exhibits a hydrophobic-hydrophilic switching property like a smart external sensing mechanism (Fig. 1b).

FT-IR and Solid-State ^{13}C NMR Analysis

FT-IR spectra of the cellulose derivatives are presented in Fig. 2a. The spectra for 6-*O*-trityl cellulose showed absorptions at: 3092.23 cm^{-1} and 3061.39 cm^{-1} for CH-aromatic; 3028.62 cm^{-1} and 2882.11 cm^{-1} (m) for CH-alkyl; 1631.04 cm^{-1}, 1600.20 cm^{-1}, and 1492.25 cm^{-1} (m) for C-C aromatic; 1447.91 (d) for C-H; and 1224.30 cm^{-1}, 1160.68 cm^{-1}, and 1058.52 cm^{-1} (m) for C-O-C (Nada *et al.* 2000; Xia *et al.* 2014; Singh *et al.* 2015). FT-IR absorptions observed for 6-*O*-trityl-2,3-*O*-acetate cellulose ester showed a broad band at around 1609.84 to 1434.42 cm^{-1} that was attributable to –COONa. The band for 2,3-*O*-acetate cellulose ester was at 1740.92 cm^{-1} for -COOH, which was mainly attributed to the conversion of -COONa to -COOH during the removal of trityl groups by acidification with concentrated HCl.

The absorption bands for 2,3-*O*-sodium acetate cellulose ester were mainly at 1604.05 cm^{-1} and 1418.99 cm^{-1} for –COONa, which was caused by treating with NaOH to convert -COOH to -COONa in order to avoid the -COOH groups reacting with heptafluorobutyryl chloride. Bands for 6-*O*-heptafluorobutyric acid-2,3-O-sodium acetate cellulose ester appeared in the absorption spectrum at: 1798.75, 1233.94, 1195.38 and 1145.26 cm^{-1}. Bands of the reaction products that were directly washed with acetone were mainly at 1742.85 cm^{-1} for -COOH, while there is no characteristic band for -CF_2-CO-. From this observation, it was concluded that the desired reaction products cannot be obtained by directly washing of the intermediate with acetone.

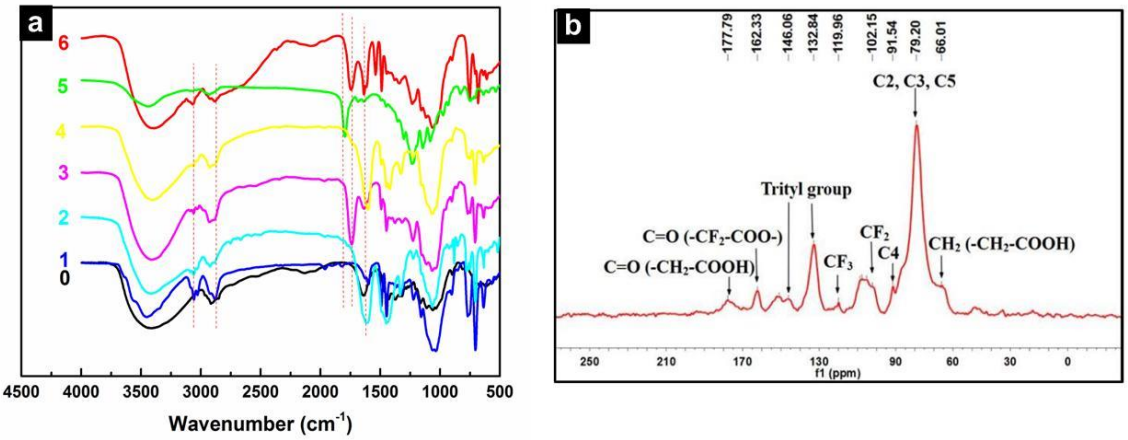

Fig. 2. (a) The FT-IR spectra of cellulose derivatives. 0. Original cellulose; 1. 6-*O*-trityl cellulose; 2. 6-*O*-trityl-2,3-*O*-acetate cellulose ester; 3. 2,3-*O*-acetate cellulose ester; 4. 2,3-*O*-sodium acetate cellulose ester; 5. 6-*O*-heptafluorobutyric acid-2,3-*O*-sodium acetate cellulose ester after DI water washings followed by acetone re-washings; 6. 6-*O*-heptafluorobutyric acid-2,3-*O*-sodium acetate cellulose ester directly washed by acetone. (b) Solid-State ^{13}C NMR spectroscopy of 6-*O*-heptafluorobutyric acid-2,3-*O*-sodium acetate cellulose ester.

The structure of the final product, 6-*O*-heptafluorobutyric acid-2,3-*O*-sodium acetate cellulose ester (product 4), was confirmed by using solid-state ^{13}C NMR analysis (Fig. 2b). Bands for the C=O structures (*e.g.*, -CH_2COOH and -CF_2COO-) where observed at 160 ppm to 180 ppm range, which indicated high degree of substitution of hydroxyl groups during derivatization. The band at approximately 80 ppm was intense and belonged to C-2, C-3, and C-5 of the *β*-D-glucopyranose unit. The ^{13}C NMR analysis suggested that there were two different functional groups, $HOOCCH_2$- and $CF_3CF_2CF_2COO$-, in the final product, which collaborate the FT-IR findings (Fig. 2a)

TGA-DTA Analysis

Selective modification of cellulose will greatly affect its thermal stability, due to disruption of the crystalline region of cellulose, molecular chain rearrangement and functional groups effects inflicted on cellulose. The thermal stability of modified cellulose has a great influence on its potential applications. Therefore, DTA-TGA analyses were conducted to characterize the derivatized material. In addition, pyrolysis components of the products were analyzed by TG-DTA-IR.

The trends observed in the DTA-TGA analyses of the cellulose derivatives are shown in Fig. 3 ((a) to (e)). After carboxylation and removal of trityl groups, the thermal degradation temperatures of the various derivatized cellulose decreased when compared to the original cellulose substrate. The maximum degradation rate temperature of cellulose, regenerated cellulose, 6-*O*-trityl cellulose and 6-*O*-heptafluorobutyric acid-2,3-*O*-sodium acetate cellulose ester is 359.4 °C, 278.8 °C, 336.9 °C, and 309.8 °C respectively. This result indicated that the introduction of large macromolecule including trityl or heptafluorobutyric group onto the cellulose chain increased the thermal stability of the cellulose derivatives, such as the resulting 6-*O*-trityl cellulose and 6-*O*-heptafluorobutyric acid-2,3-*O*-sodium acetate cellulose ester. The thermal stabilities of the cellulose, the trityl cellulose, and the final product samples are also shown in Fig. 3 (f). From room temperature to 150 °C, the weight loss of the original cellulose substrate was 4.28%, whereas there was almost no mass loss of 6-*O*-trityl cellulose. When the temperature increased to 600 °C, the weight loss of cellulose was much higher than that of 6-*O*-heptafluorobutyric acid-2,3-*O*-sodium acetate cellulose ester, which indicated that the structure of the modified cellulose is different from the original cellulose substrate. It was concluded that selective modification of cellulose affected the heat resistance and thermal stability of the cellulose backbone.

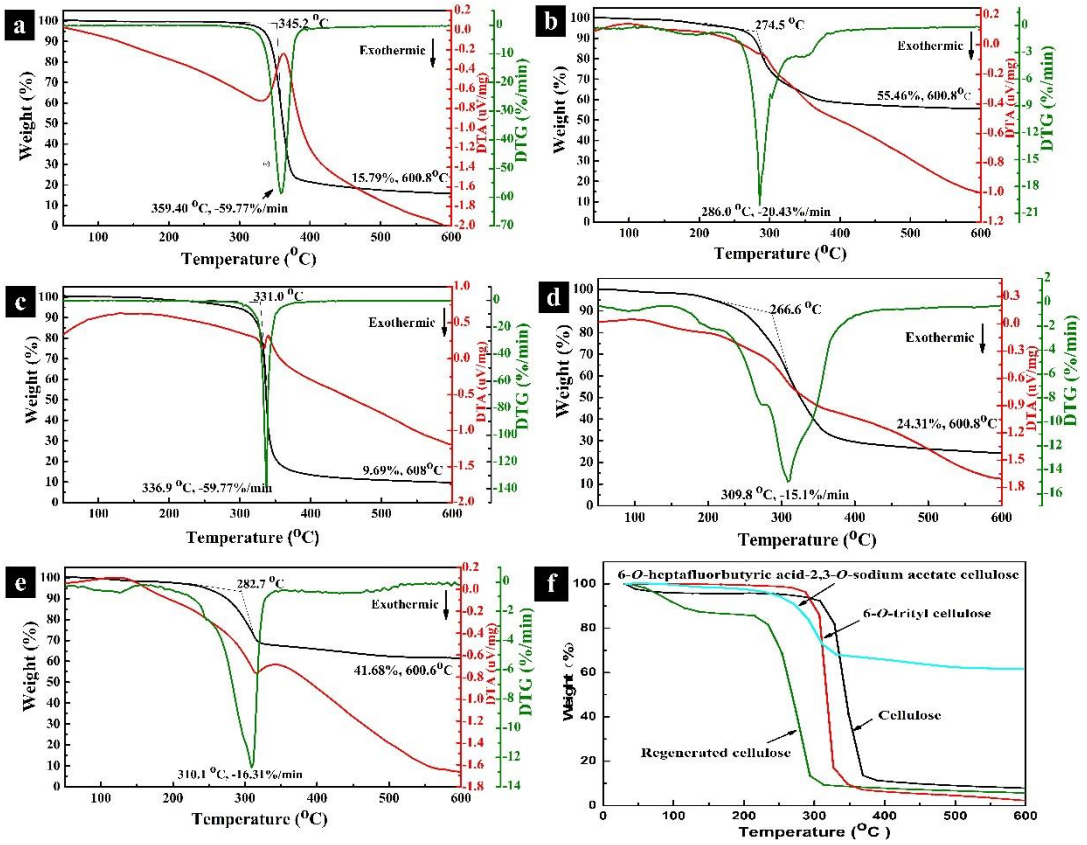

Fig. 3. DTA-TGA of cellulose and cellulose derivatives: (a) cellulose; (b) 2,3-*O*-sodium acetate cellulose ester; c) 6-*O*-trityl cellulose; (d) 6-*O*-heptafluorobutyric acid-2,3-*O*-sodium acetate cellulose ester; (e) 6-*O*-trityl-2,3-*O*-acetate cellulose ester; and (f) TGA of cellulose and cellulose derivatives.

Contact Angle and Microstructure of Surface HHSCMs

A sheet prepared with the final derivatized cellulose (6-*O*-heptafluorobutyric acid-2,3-*O*-sodium acetate cellulose ester) was examined for its hydrophobicity and oleophobicity using dynamic contact angle measurements (Fig. 4). When a droplet of pure water was placed onto the surface of the sample, its contact angle was 103°, which indicated the material was initially hydrophobic. However, the surface contact angle decreased significantly from 103° to 73° after 5 min of contact at ambient temperature (19.8 °C) and relative humidity (65%). After 5 min, the sample surface showed significant hydrophilicity (Fig. 4a). As contact time increased, the water droplets on the sample surface gradually infiltrated and penetrated until internal cellulose finished the absorbing and swelling process, which turned the original flat surface into a parabolic convexity (Fig. 4c). This indicated that the physical structure of the substrate had changed significantly. However, when conducting an oleophobic test by applying a droplet of CH_2I_2, the contact angle was 106°. The contact angle and material morphology did not change over time, which indicated the substrate was oleophobic. The physical structure of the substrate did not change during the oleophobic test (Fig. 4b). The decreasing curve of contact angles given in Fig. 4d further manifested these macromolecular cellulosic materials met expectations of self-switching ability between oleophobic-hydrophobic and hydrophilic.

Since the contact angles with both water and methylene iodide were measured, it was then possible to calculate the surface free energy by the Owens-Wendt-Rabel-Kaelble (OWRK) method. The OWRK method is used when investigating the effect of polar and disperse interactions on wettability and adhesion. The result indicated that the surface free energy had obviously changed. After wetting, dispersion components of surface free energy decreased from 4.31 to 1.16 J·m, while the polarity components of surface free energy increased from 6.72 to 32.11 J·m.

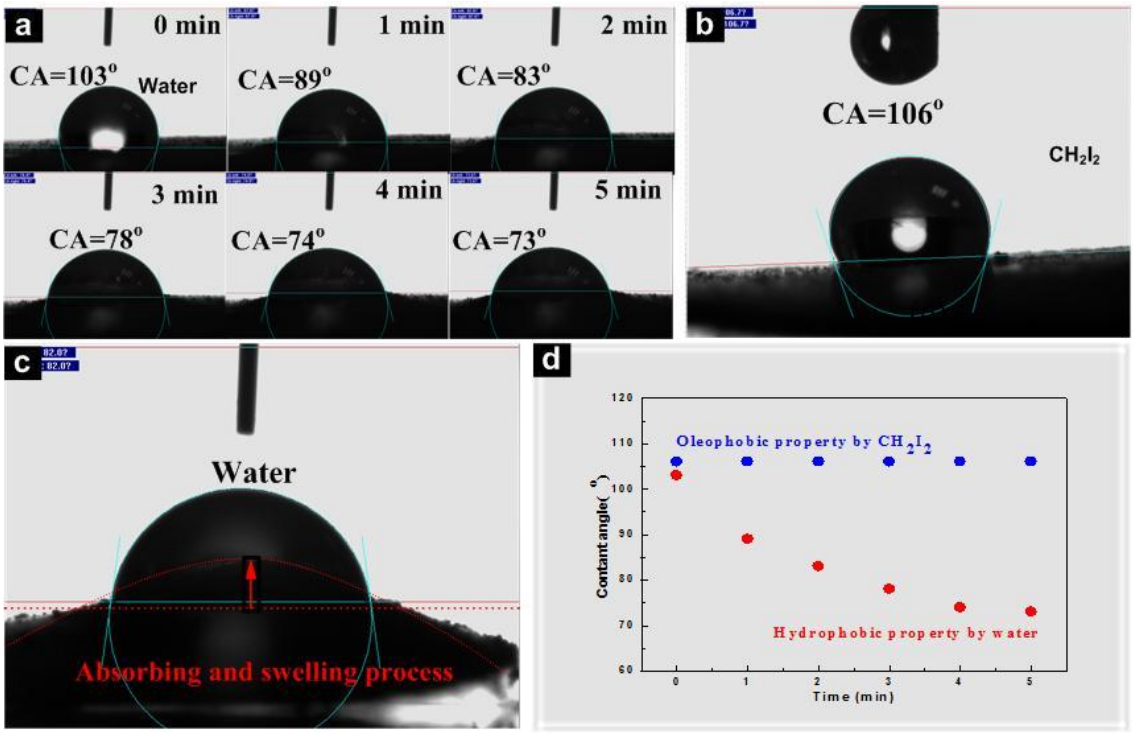

Fig. 4. (a) Water contact angle on the surface of HHSCMs samples; (b) CH2I2 contact angle on the surface of HHSCMs samples; (c) microstructure of surface swelling after absorbing water; and (d) change in contact angles over time for water and CH_2I_2 drop tests

Element Components Measured by XPS

XPS analyses were conducted at two different incident contact angles of 0° and 55° in order to further observe the physico-chemical surface changes of the HHSCM and to elucidate the mechanism of the hydrophilic/hydrophobic switching. At 0°, the chemical composition of the inner coating was measured, while the outer layer was measured at 55°.

The final product contains F, O, and C atoms, which corresponds to the derivatizing groups at C-2, C-3, and C-6 positions on the cellulose (Fig. 5).

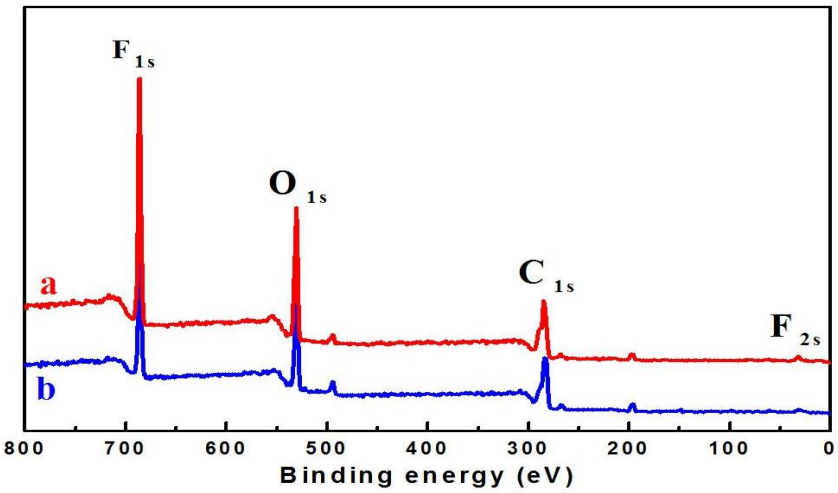

Fig. 5. Total XPS of 6-*O*-heptafluorobutyric acid-2,3-*O*-sodium acetate cellulose ester sheet (HHSCM): (a) dry, and (b) wet

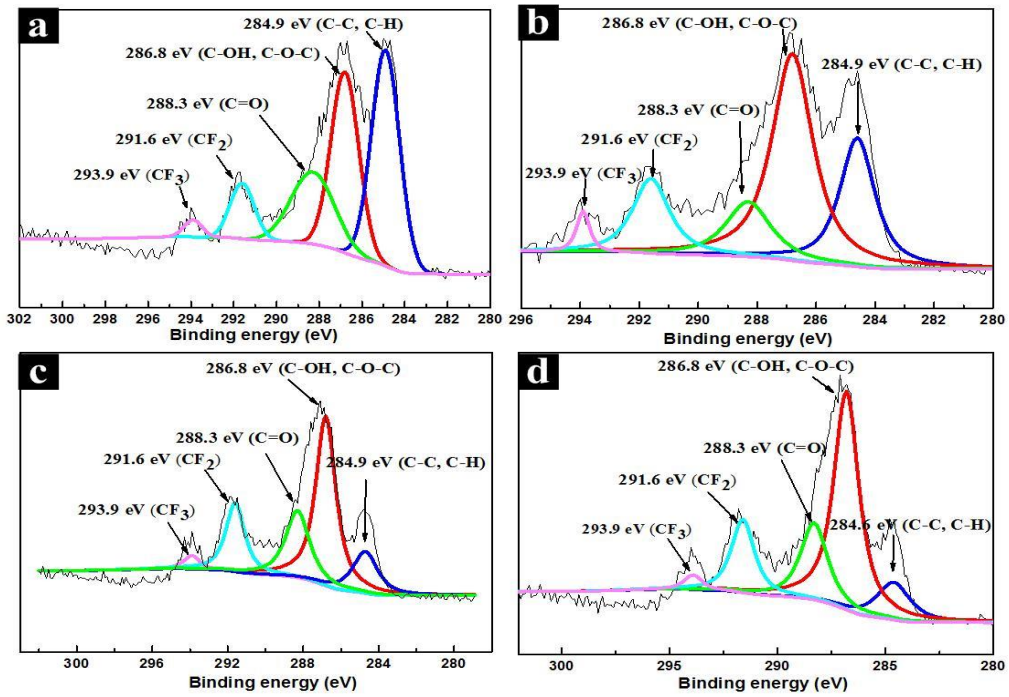

Fig. 6. O_{1s}, C_{1s} and F_{2s} XPS of 6-*O*-heptafluorobutyric acid-2,3-*O*-sodium acetate cellulose ester sheet: (a) O_{1s}, C_{1s}, and F_{2s} XPS (0°; dry); (b) O_{1s}, C_{1s}, and F_{2s} XPS (55°; dry); (c) O_{1s}, C_{1s}, and F_{2s} XPS (0°; wet); (d) O_{1s}, C_{1s}, and F_{2s} XPS (55°; wet);

The XPS analyses showed that the peak of C_{1s} is mainly found in C_{1s1}, C_{1s2}, and C_{1s3}. The peak of O is mainly found in O_{1s1} and O_{1s2}. The binding energies of C_{1s1}, C_{1s2}, and C_{1s3} are mainly found at 284.9 eV, 286.8 eV, and 288.3 eV, respectively, while the binding energies of CF_2 and CF_3 are found at 291.6 eV and 293.9 eV, respectively. C_{1s1} peak represents -C-H or -C-C, C_{1s2} peak represents of -C-O, and C_{1s3} represents -COOH. CF_2 and CF_3 are mainly the fluorine-containing oleophobic-hydrophobic functional groups (Figs. 6 and 7).

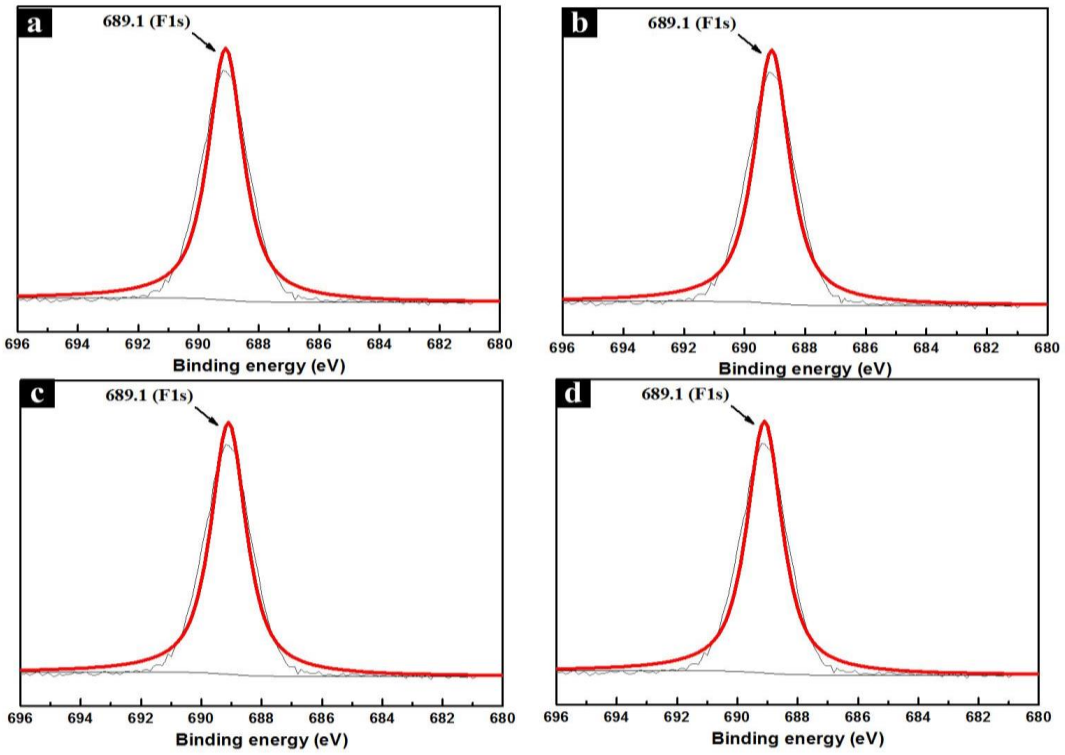

Fig. 7. F_{1s} XPS of 6-*O*-heptafluorobutyric acid-2,3-*O*-sodium acetate cellulose ester sheet: (a) 0°, dry; (b) 55°, dry; (c) 0°, wet; (d) 55°, wet

The changes in the XPS before and after wetting at 0° and 55° can be seen by deconvoluting the peak area for each atomic component. Table 1 shows that the individual contributions of deconvoluted components changed at different depths within HHSCM before and after wetting. After wetting, the surface free energy had obviously changed. The surface free energy increased from 11.03 to 34.09 J·m, of which the polarity component increased from 60.92% to 94.19%. This indicated that the polar groups migrated to the material surface after wetting. The change can be attributed to an increase of polar groups on the surface, such that the surface became hydrophilic and the surface free energy increased. The HHSCM assembled by 6-*O*-heptafluorobutyric acid-2,3-*O*-sodium acetate cellulose ester has a very strange spatial chemical structure with hydrophobic and hydrophilic groups on opposite sides of the cellulose backbone. The results agree well with the results from IR spectra.

Table 1. XRF Peak Area and Ratio Values of Elemental Components Determined at Contact Angles of 0°and 55° for the HHSCM

Peak Area							Ratio Values		
Material State	C-C, C-H	C-OH	C=O	CF_2	CF_3	Total F	CF_3/COOH	CF_2/COOH	F/COOH
Dry (0°)	5688	4719	2898	1254	290	38130	0.10	0.43	13.16
Dry (55°)	3354	6320	1832	2043	403	32309	0.22	1.12	17.64
Wet (0°)	2274	7397	3465	2811	471	55396	0.14	0.81	15.98
Wet (55°)	1419	6262	2372	1942	309	38927	0.13	0.82	16.41

First, the incident angle at 55° was taken as a method for determining the chemical elements at the surface layer of the HHSCM. The peak area ratio values corresponding to CF_3, CF_2, and total F, which contain the oleophobic-hydrophobic group (CF_3-CF_2-CF_2-CO-) and the hydrophilic group (HOOC-), were 0.22, 1.12, and 17.64, respectively, before wetting, while the ratio values decreased to 0.13, 0.82, and 16.41, respectively, after wetting. This observation indicated that the content of oleophobic-hydrophobic groups at the exposed surface decreased after wetting, while the hydrophilic HOOC- groups increased.

The incident angle at 0° was taken as a method for determining the chemical elements in the inner layer of the HHSCM. The peak area ratio values corresponding to CF_3, CF_2, and total F, which contain the oleophobic-hydrophobic groups (CF_3-CF_2-CF_2-CO-) and hydrophilic (HOOC-), were 0.10, 0.43, and 13.16, respectively, before wetting, while the ratios values increased to 0.14, 0.81, and 15.98 after wetting. This indicated that the content of oleophobic-hydrophobic groups in the interior increased after wetting, while the hydrophilic HOOC- groups decreased.

CONCLUSIONS

1. A switchable hydrophobic/hydrophilic surface was successfully prepared by modifying the cellulose biopolymer by regioselective functionalization grafting of oleophobic-hydrophobic and hydrophilic groups. Groups with hydrophobic and hydrophilic properties were grafted on opposite sides of the cellulose backbone; the groups are designed to reorient themselves to lower the surface energy when the external environment changed.
2. The hydrophobic/hydrophilic switchable cellulosic surface displayed excellent thermal stability compared to regenerated cellulose and conversion sensitivity. After wetting, the dispersion component of surface free energy decreased, while the polarity component of surface free energy increased. Furthermore, the synthesis process by regioselective functionalization with an ionic liquid solvent provided a new and effective strategy for manufacturing stable, environmentally sustainable hydrophobic/hydrophilic surfaces for industrial applications.

ACKNOWLEDGMENTS

This work was financially supported by the State Key Laboratory of Pulp and Paper Engineering (Grant No. 2016C08), Guangzhou Science and Technology Plan Project (Grant No. 201704030066), Guangdong Province Youth Science and Technology Innovation Talents (Grant No. 2014TQ01C781), Science and Technology Planning Project of Guangdong Province, China (Grant No. 2016B090918074), and the Fundamental Research Funds for the Central Universities, South China University of Technology (Grant No. 2017ZD087).

REFERENCES CITED

Fox, S. C., Li, B., Xu, D., and Edgar, K. J. (2011). "Regioselective esterification and etherification of cellulose: A review," *Biomacromolecules* 12(6), 1956-72. DOI: 10.1021/bm200260d

Godeau, G., Darmanin, T., and Guittard, F. (2016). "Switchable surfaces from highly hydrophobic to highly hydrophilic using covalent imine bonds," *J. Appl. Polym. Sci.* 133(11), 43130. DOI: 10.1002/app.43130

Granström, M., Olszewska, A., Mäkelä, V., Heikkinen, S., and Kilpeläinen, I. (2009). "A new protection group strategy for cellulose in an ionic liquid: Simultaneous protection of two sites to yield 2,6-di-O-substituted mono- p-methoxytrityl cellulose," *Tetrahedron Lett.* 50(15), 1744-1747. DOI: 10.1016/j.tetlet.2009.01.144

Gupta, K. M., and Jiang, J. (2015). "Cellulose dissolution and regeneration in ionic liquids: A computational perspective," *Chem. Eng. Sci.* 121(6 Jan. 2015), 180-189. DOI: 10.1016/j.ces.2014.07.025

Heinze, T., and Liebert, T. (2001). "Unconventional methods in cellulose functionalization," *Prog. Polym. Sci*. 26(9), 1689-1762. DOI: 10.1016/S0079-6700(01)00022-3

Iriyama, Y. (2010). "Surface treatment of hydrophobic polymers by atmospheric-pressure plasma," *J. Photopolym. Sci. Technol.* 23(4), 599-603. DOI: 10.2494/photopolymer.23.599

Kamitakahara, H., Funakoshi, T., Nakai, S., Takano, T., and Nakatsubo, F. (2010). "Synthesis and structure/property relationships of regioselective 2-O-, 3-O- and 6-O-ethyl celluloses," *Macromol. Biosci.* 10(6), 638. DOI: 10.1002/mabi.200900392

Klemm, D., Heublein, B., Fink, H. P., and Bohn, A. (2005). "Cellulose: Fascinating biopolymer and sustainable raw material," *Angew. Chem.* 44(22), 3358-3393. DOI: 10.1002/anie.200460587

Koschella, A., Fenn, D., Illy, N., and Heinze, T. (2006). "Regioselectively functionalized cellulose derivatives: A mini review," *Macromol. Symp*. 244(1), 59-73. DOI: 10.1002/masy.200651205

Liu, D., Li, J., Yang, R., Mo, L., Huang, L., Chen, Q., and Chen, K. (2008). "Preparation and characteristics of moulded biodegradable cellulose fibers/MPU-20 composites (CFMCs) by steam injection technology," *Carbohyd. Polym*. 74(2), 290-300. DOI: 10.1016/j.carbpol.2008.02.015

Liu, D., Xia, K., and Yang, R. (2012). "Synthetic pathways of regioselectively substituting cellulose derivatives: A review," *Curr. Org. Chem*. 16(16), 1838-1849. DOI: 10.2174/138527212802651269

Long, M., Peng, S., Chen, J., Yang, X., and Deng, W. (2016). "A new replication method for fabricating hierarchical polymer surfaces with robust superhydrophobicity and highly improved oleophobicity," *Colloid. Surf. A* 507(20 Oct. 2016), 7-17. DOI: 10.1016/j.colsurfa.2016.07.085

Luby, P., Kuniak, Ľ., and Fanter, C. (2003). "Crosslinking statistics, 3. Relation between relative reactivity and accessibility of cellulose hydroxyl groups," *Makromolekul. Chem.* 180(10), 2379-2386. DOI: 10.1002/macp.1979.021801012

Nada, A., Dawy, M., and Shabaka, A. (2000). "Molecular structure and electrical insulating properties of grafted and cyanoethylated cellulose," *International Journal of Polymeric Materials & Polymeric Biomaterials* 47(2-3), 195-206. DOI: 10.1080/00914030008035060

Owens, D. K., and Wendt, R. C. (1969). "Estimation of the surface free energy of polymers," *Appl. Polym. Sci.* 13, 1741-1747. DOI: 10.1002/app.1969.070130815

Pinkert, A., Marsh, K. N., and Pang, S. (2010). "Reflections on the solubility of cellulose," *Ind. Eng. Chem. Res*. 49(22), 11121-11130. DOI: 10.1021/ie1006596

Pinkert, A., Marsh, K. N., Pang, S., and Staiger, M. P. (2009). "Ionic liquids and their interaction with cellulose," *Chem. Rev*. 109(12), 6712-28. DOI: 10.1021/cr9001947

Raghavanpillai, A., Franco, V. A., and Meredith, W. E. (2012). "Hydrophobic and oleophobic surface modification using gelling agents derived from amino acids," *J. Fluorine Chem.* 135(March 2012), 187-194. DOI: 10.1016/j.jfluchem.2011.10.015

Roy, D., Semsarilar, M., Guthrie, J. T., and Perrier, S. (2009). "Cellulose modification by polymer grafting: A review," *Chem. Soc. Rev.* 38(7), 2046-2064. DOI: 10.1039/b808639g

Rudawska, A., and Jacniacka, E. (2009). "Analysis for determining surface free energy uncertainty by the Owens–Wendt method," *International Journal of Adhesion & Adhesives* 29(4), 451-457. DOI: 10.1016/j.ijadhadh.2008.09.008

Ryu, H. Y., Yoon, S. H., Han, D. H., Hafeez, H., Paluvai, N. R., Lee, C. S., and Park, J. G. (2016). "Fabrication of hydrophobic/hydrophilic switchable aluminum surface using poly(N -isopropylacrylamide)," *Prog. Org. Coat*. 99(Oct. 2016), 295-301. DOI: 10.1016/j.porgcoat.2016.06.008

Sawada, E., Kakehi, H., Chounan, Y., Miura, M., Sato, Y., Isu, N., and Sawada, H. (2010). "UV-induced switching behavior of novel fluoroalkyl end-capped vinyltrimethoxy-silane oligomer/titanium oxide nanocomposite between superhydrophobicity and superhydrophilicity with good oleophobicity," *Compos. Part B - Eng.* 41(6), 498-502. DOI: 10.1016/j.compositesb.2010.04.002

Schaller, J., and Heinze, T. (2005). "Studies on the synthesis of 2,3-O-hydroxyalkyl ethers of cellulose," *Macromol. Biosci*. 5(1), 58-63. DOI: 10.1002/mabi.200400136

Shen, T., and Gnanakaran, S. (2009). "The stability of cellulose: A statistical perspective from a coarse-grained model of hydrogen-bond networks," *Biophys. J*. 96(8), 3032-3040. DOI: 10.1016/j.bpj.2008.12.3953

Singh, R. K., Gupta, P., and Sharma, O. P. (2015). "Homogeneous synthesis of cellulose fatty esters in ionic liquid (1-butyl-3-methylimidazolium chloride) and study of their comparative antifriction property," *Journal of Industrial & Engineering Chemistry* 24, 14-19. DOI:10.1016/j.jiec.2014.09.031

Tang, S., Li, X., and Wang, F., Liu, G., Li, Y., Pan, F. (2012). "Synthesis and HPLC chiral recognition of regioselectively carbamoylated cellulose derivatives," *Chirality* 24(2), 167. DOI: 10.1002/chir.21978

Tsunashima, Y., Hattori, K., Kawanishi, H., and Horii, F. (2001). "Regioselectively substituted 6-O- and 2,3-di-O- acetyl-6-O- triphenylmethylcellulose: Its chain dynamics and hydrophobic association in polar solvents," *Biomacromolecules* 2(3), 991-1000. DOI: 10.1021/bm010069e

Van Oss, C. J. (1995). "Hydrophobic, hydrophilic and other interactions in epitope-paratope binding," *Mol. Immunol*. 32(3), 199-211. DOI: 10.1016/0161-5890(94)00124-J

Vitz, J., Erdmenger, T., Haensch, C., and Schubert, U. S. (2009). "Extended dissolution studies of cellulose in imidazolium based ionic liquids," *Green Chem*. 11(3), 417-424. DOI: 10.1039/b818061j

Wang, C., Tan, H., Dong, Y., and Shao, Z. (2006). "Trimethylsilyl hydroxypropyl cellulose: Preparation, properties and as precursors to graft copolymerization of e-

caprolactone," *React. Funct. Polym.* 66(10), 1165-1173. DOI: 10.1016/j.reactfunctpolym.2006.02.006

Xia, K., Chen, J., Yang, R.,Cheng F., and Liu, D. (2014). "Green synthesis and crystal structure of regioselectively substituting 6-O-tritylcellulose derivatives," *Journal of Biobased Materials & Bioenergy* 8(6), 587-593(7). DOI:10.1166/jbmb.2014.1472

Yuan, H., Chi, H., and Yuan, W. (2016). "Ethyl cellulose amphiphilic graft copolymers with LCST-UCST transition: Opposite self-assembly behavior, hydrophilic-hydrophobic surface and tunable crystalline morphologies," *Carbohyd. Polym.* 147(20 Aug. 2016), 261-271. DOI: 10.1016/j.carbpol.2016.04.013

Yue, M., Zhou, B., Jiao, K., Qian, X., Xu, Z., Teng, K., Zhao, L., Wang, J., and Jiao, Y. (2015). "Switchable hydrophobic/hydrophilic surface of electrospun poly (l-lactide) membranes obtained by CF_4 microwave plasma treatment," *Appl. Surf. Sci.* 327(30 April 2015), 93-99. DOI: 10.1016/j.apsusc.2015.01.145

Zhang, K., Peschel, D., Klinger, T., Gebauer, K., Groth, T., and Fischer, S. (2010). "Synthesis of carboxyl cellulose sulfate with various contents of regioselectively introduced sulfate and carboxyl groups," *Carbohyd. Polym.* 82(1), 92-99. DOI: 10.1016/j.carbpol.2010.04.027

Zheng, X., Xu, D., and Edgar, K. J. (2015). "Cellulose levulinate: A protecting group for cellulose that can be selectively removed in the presence of other ester groups," *Cellulose* 22(1), 301-311. DOI: 10.1007/s10570-014-0508-8

Article submitted: October 11, 2017; Pee review completed: December 4, 2017; Revised version received: Decmeber 21, 2017; Accepted: December 27, 2017; Published: January 9, 2018.
DOI: 10.15376/biores.13.1.1475-1490